ELSEVIER

Nuclear Instruments and Methods in Physics Research A 470 (2001) 145–154

NUCLEAR INSTRUMENTS & METHODS IN PHYSICS RESEARCH Section A

www.elsevier.com/locate/nima

An experimental study of the $q_\perp$-dependence of X-ray resonant diffuse scattering from multilayers

V.A. Chernov[a], V.I. Kondratiev[b], N.V. Kovalenko[b], S.V. Mytnichenko[c,*]

[a] *Siberian SR Centre, Budker Institute of Nuclear Physics, 11 Lavrentyev Ave., 630090 Novosibirsk, Russia*
[b] *Budker Institute of Nuclear Physics, 11 Lavrentyev Ave., 630090 Novosibirsk, Russia*
[c] *Institute of Solid State Chemistry, 18 Kutateladze Str., 630128 Novosibirsk, Russia*

Abstract

A study of X-ray resonant diffuse scattering from the W/Si multilayer was performed to examine its dependence on the momentum transfer normally to the specular diffraction plane, $q_\perp$. The data obtained show two evident disagreements with the present theoretical approximations. Firstly, when the incident angle was approximately equal to the Bragg angle, additional scattering concentrated in the specular diffraction plane was observed. Secondly, the $q_\perp$-dependence of the quasi-Bragg scattering intensity obtained from these experiments is not the same, at least at the small momentum transfer, as can be obtained from the scans in the specular diffraction plane, having tendency to accumulate near this plane. The possible reasons for these phenomena are discussed.

PACS: 68.55. − a; 61.10.Kw

Keywords: Multilayers; X-ray diffuse scattering

1. Introduction

Thin films composed of synthetically-grown multilayer structures represent a new class of materials having novel optical, electric, magnetic, and superconducting properties for a host of important applications. Since the properties of a multilayer principally differ from those of bulk materials, it is not a surprise that these properties are often highly sensitive to the nature of layer interfaces. Thus, in order to understand and control physical behavior of multilayers, it is essential to be able to determine the detailed structure of layers and interfaces and to correlate this structure with the measured physical properties.

A promising technique for characterizing the roughness of surfaces and interfaces in multilayer structures is X-ray diffuse scattering. This structural method has advantages that prove its usefulness. It is a non-invasive technique, well suited for dynamic measurements, including in situ growth studies. Large depth penetration of X-rays provides bulk structural information, including the cross-correlation effects. Structural information can be obtained over a wide spatial range, from macroscopic (0.1–100 μm) down to atomic

*Corresponding author. Siberian SR Centre, Budker Institute of Nuclear Physics, 11 Lavrentyev Ave., 630090 Novosibirsk, Russia. Tel.: +7-3832-394013; fax: +7-3832-394163.

E-mail address: s.v.mytnichenko@inp.nsk.su (S.V. Mytnichenko).

0168-9002/01/$ - see front matter
PII: S0168-9002(01)01031-2

dimensions. The diffuse scattering data are averaged over the sample area, which makes this technique complementary, for example, for atomic force microscopy.

In spite of these advantages, diffuse scattering as a technique for investigation of a multilayer interfacial structure is not widely used now. (In this paper, only the case when the total integrated diffuse scattering intensity is much smaller than the specular reflection one will be discussed. This condition is equivalent to $\sigma < \Lambda/n$, where σ is the roughness dispersion, Λ is the multilayer period, and n is Bragg order [1].) The reason is both the experimental and data interpretation difficulties. Indeed, in contrast to specular diffraction, X-ray diffuse scattering occurs at any direction including the specular one due to the violation of multilayer lateral translation symmetry by the roughness imperfections. At the same time, only a combination of the specular and off-specular scattering measurements provides full structural information on the surfaces and interfaces. Thus, even though multilayer interfacial roughness anisotropy is unavailable, it is necessary to obtain a diffraction space map instead of a standard one-dimensional scan. Roughness anisotropy of this sort will cause the technique sophistication to further increase. For a variety of reasons, diffuse scattering undergoes resonant amplification and is brought into the relatively small angle regions near the specular Bragg reflections forming its setting.

A standard diffuse scattering experiment represents a set of one-dimensional scans in the specular diffraction plane, with that another degree of integration in the direction normal to it (see Fig. 1). It may be noted that the intensity distribution in this direction is automatically assumed to be independent of the incident and scattering angles. A typical image of a Bragg reflection fine structure obtained by such experiments is schematically shown in Fig. 2. The following distinguishing features of resonant diffuse scattering can be observed:

The incoming and *outgoing Bragg-enhanced diffuse scattering* manifests itself as a resonant amplification of diffuse scattering in the case of

$$\theta_0 \approx \theta_B \text{ or } \theta_1 \approx \theta_B \tag{1}$$

where θ_B is the Bragg angle. This dynamic phenomenon was observed experimentally by several authors [1,2] and can be explained within the framework of the distorted-wave Born approximation [3–5]. According to this approximation, in the case of complete correlation between roughness of different layers (cross-correlation) [6], the contribution from this scattering to the total scattering amplitude has the form

$$A_{\text{incoming}} \sim R_0 \Phi(\Delta\psi) \quad \text{and} \quad A_{\text{outgoing}} \sim R_1 \Phi*(\Delta\psi) \tag{2}$$

where R_0 and R_1 are the specular reflection amplitude at the incident angles θ_0 and θ_1,

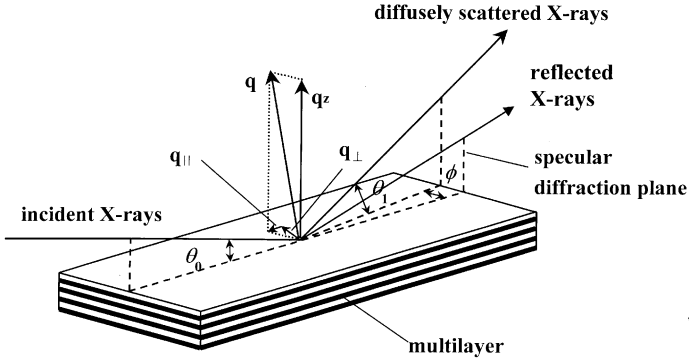

Fig. 1. The diffuse scattering geometry: θ_0 and θ_1 are the incident and diffracted angles, respectively; $\omega = \theta_0$-θ_1; ϕ is the azimuthal angle; q_z is the momentum transfer normal to the lateral planes; $q_\parallel$ is the momentum transfer parallel to the lateral planes and specular diffraction plane; $q_\perp$ is the momentum transfer parallel to the lateral planes and normal to the specular diffraction plane.

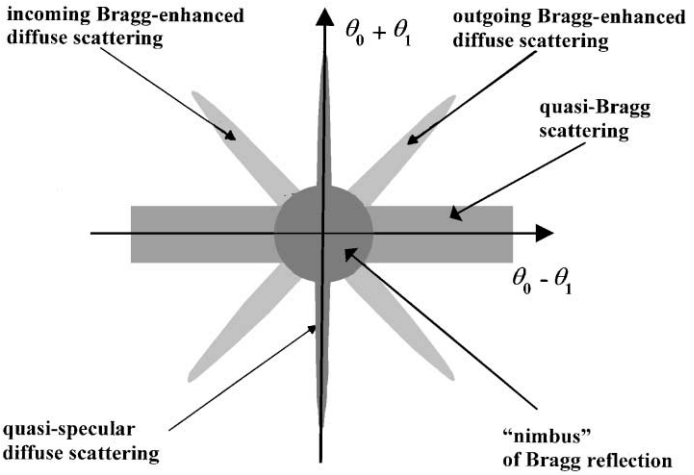

Fig. 2. The fine structure of the Bragg reflection from a multilayer as may be observed in any standard diffuse scattering experiment. Here the sets of transverse scans (ω-scans) are parallel to the ordinate axis, whereas the total diffraction angles are plotted along the vertical axis.

respectively; $\Delta\psi = \psi_0 - \psi_1$; ψ is the phase shift of the wave as it passed through one multilayer period; $\Phi(\xi) = (1 - e^{iN\xi})/(1 - e^{i\xi})$ is the usual diffraction function and N is the number of multilayer periods. If the roughness cross-correlation is absent, the mechanism of Bragg-enhanced diffuse scattering is analogous to appearance of fluorescent Kossel lines. It should be noted that not only the resonant amplification lines can be observed, but also the breaks in a diffuse scattering background [1]. The smaller is the roughness cross correlation, the better is to observe this effect, caused by the specular diffraction standing wave.

Apart from condition (1), the scattering amplitudes A_{incoming} and A_{outgoing} are subjected to resonant amplification if

$$\theta_0 \approx \theta_1 \quad \text{or} \quad \Delta\psi \approx 0. \tag{3}$$

Quasi-specular diffuse scattering is caused by this amplification.

Besides, the additional term with the resonant condition

$$\theta_0 \approx \theta_1 \approx \theta_B \tag{4}$$

provides diffuse scattering near the Bragg point, forming the "*Bragg nimbus*".

Finally, *quasi-Bragg scattering* was theoretically predicted in 1988 [7]. In contrast to other types of diffuse scattering, quasi-Bragg scattering is not caused by dynamic effects but only by diffraction of X-rays from the interfacial imperfections coherently repeating from one layer to another (the interfacial cross-correlation) [6,7]. Indeed, due to the translation symmetry normally to the multilayer surface, the momentum transfer projection on this axis must be kept with an accuracy of $2\pi/\Lambda$, where Λ is the translation symmetry or multilayer period. It makes possible to immediately obtain the quasi-Bragg condition

$$\theta_0 + \theta_1 \approx n2\theta_B. \tag{5}$$

This condition means that the scattering occurs at the total scattering angle $n2\theta_B$ beyond any incident angle. The condition accuracy is determined by the multilayer rocking curve.

The origin of quasi-Bragg scattering can be explained by a more illustrative method [8]. Condition (5) is neither more nor less than the reflection condition of diffraction from a grating that is not coincidental. Fig. 3 demonstrates that quasi-Bragg diffuse scattering is caused by diffraction from a grating placed normally to the interfaces and composed by interfacial imperfections coherently repeating from one layer to another. The multilayer and grating periods are evidently the same.

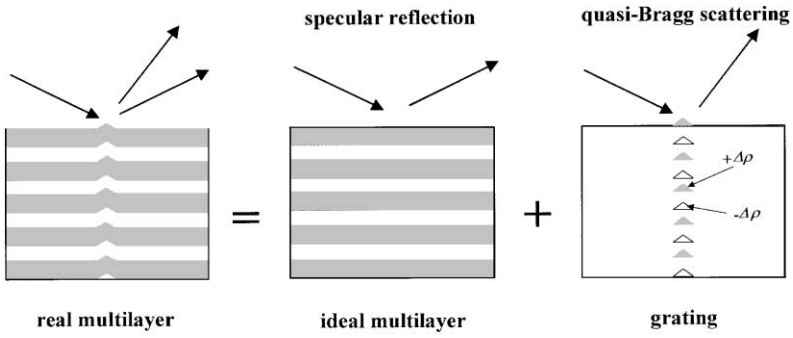

Fig. 3. The nature of quasi-Bragg diffuse scattering.

These properties of quasi-Bragg diffuse scattering significantly simplify its theoretical descriptions, especially, when the incident angle is not equal to the Bragg angle. In this case the nature of quasi-Bragg scattering is clearly kinematic, and its intensity distribution versus the momentum transfer is directly proportional to the power spectral density of interfacial roughness omitting the cross-correlation effects. Under these conditions, the $q_\perp$-dependence of the quasi-Bragg diffuse scattering reflects directly the roughness power spectral density as well as the $q_\parallel$-dependence [9].

All theories of resonant diffuse scattering based on the distorted-wave Born or kinematic approximations predict the same $q_\perp$-dependence independently of the diffraction nature (kinematic or dynamic) and type of diffuse scattering, if the interfacial roughness is assumed to be isotropic in the lateral planes. Moreover, as it was mentioned above, $q_\perp$- and $q_\parallel$-dependences must be equivalent in the kinematic approximation. However, from our point of view, the latter effect is not a universal physical law and is caused by the use of the self-affine roughness model by Sinha et al. [10] with height–height self-correlation function of the form

$$C(r) = <z(\boldsymbol{r}')z(\boldsymbol{r}'+\boldsymbol{r})> = \sigma^2\exp(-(r/\xi)^{2h}) \qquad (6)$$

where σ is the rms roughness, ξ is the correlation length, and h is a coefficient connected with the fractal dimension $D = 3-h$. Indeed, the choosing of correlation function (6) means automatically that the roughness imperfections have a point nature, i.e. are spatially restricted in all lateral directions (if $r \to \infty$ then $C(r) \to 0$). So, a great class of roughness imperfections which do not obey condition (6) is omitted from the consideration. Nevertheless, it is reasonable to assume existence of another type of imperfections that are unlimited in some lateral directions. The case of linear defects due to various physical and technological reasons is of special interest. The diffuse scattering from these roughness imperfections will be concentrated near the specular diffraction plane, which is easy to show. In other words, in this case the diffuse scattering behavior in the specular diffraction plane will not strongly differ from the theoretically predicted one, but at the same time the $q_\perp$-dependence of resonant diffuse scattering will alternate, having the tendency to accumulate near the specular diffraction plane.

Besides, interfacial roughness was shown by the atomic-force microscopy [11] to have not one but a few characteristic lengths in various spatial ranges. The roughness imperfections of different spatial ranges are caused by different physical reasons and must have different correlation functions.

In the present work an experimental study of the $q_\perp$-dependence of resonant diffuse scattering was performed.

2. Experimental

The W/Si multilayer was deposited by magnetron sputtering on a flat silica wafer with a surface roughness of 0.3–0.5 nm. The number of bilayers was 200. A least-squares fitting of the experimental specular reflectivity data was performed to

calculate the multilayer optical parameters using Parrat's recursive dynamical method [12]. Below are the multilayer parameters obtained. The multilayer period, Λ, was 1.47 nm. The W-rich layer comprised approximately 0.5 of this period. The roughness parameter, σ, was found to be equal to 0.6 nm. (This value reflects both macro-roughness and presence of mixed layers.)

The X-ray diffuse scattering measurements were performed using SR of the VEPP-3 storage ring of the Siberian SR Centre at Budker INP, which operates at 2 GeV and with a maximum stored current of 165 mA. A triple-axis diffractometer (Fig. 4a) with a primary channel-cut single-crystal Si(1 1 1) monochromator and a Ge(1 1 1) crystal-collimator of the "anomalous scattering" station were used [13]. The measured angular broadening of the diffractometer had a full-width at half-maximum (FWHM) of 15″. A scintillation detector based on an FEU-130 photomultiplier with a NaI(Tl) scintillator was used. The dynamic range of the detector system was about 5×10^4. To increase the dynamic range of the measurements up to about 10^7, calibrated copper fails were used to alternate the incident beam. In order to perform the $q_\perp$-experiments the additional horizontal slits, providing an azimuthal angle resolution about 0.05°, were used.

Besides, for the study of quasi-Bragg scattering, an experimental scheme with an image plate was used (Fig. 4b).

The measurements were performed at the wavelength $\lambda = 0.154$ nm.

3. Bragg-enhanced diffuse scattering

The diffraction space map of the first Bragg reflection obtained by the conventional method is shown in Fig. 5a: the horizontal strip is the quasi-Bragg scattering, the inclined strips are the incoming and outgoing Bragg-enhanced diffuse scattering. Such a strip rich pattern is caused by the fact that every Kiessig modulation has its own quasi-Bragg sheet and Bragg-enhanced diffuse scattering strips.

The main difference between the maps in Fig. 5a and 2 is the intensity asymmetry of the incoming and outgoing Bragg-enhanced diffuse scattering. According to the distorted-wave Born approximation as well as other theoretical calculations [14], these intensities must be symmetrical relative to the specular vertical line, omitting the trivial geometry factor. Moreover, this symmetry seems to be stated by the optics reciprocity theorem. Indeed, it seems that the intensities must be equal if the infinitely distant source and detector are replaced. Nevertheless, from our point of view, the optics reciprocity theorem cannot be true in the case of statistical systems, since this theorem is a direct consequence of symmetry of Maxwell's equations relative to the time reverse. Statistical averaging breaks this symmetry. Another important condition is the fact that the incident beam does not represent the ideal plane monochromatic wave but a wave packet having limited space sizes.

"To be sure that the discussed phenomenon is not an experimental artifact we tried to replace the crystal-collimator with vertical slits and to use additional collimators, with no any success. It is necessary to mark that the anomalous high intensity of incoming Bragg enhanced diffuse scattering was observed in Ref. [15], where the small-angle Bragg reflections from a semiconductor superlattice were studied. The experimental scheme of this work principally differs from the scheme discussed here. In our previous work devoted to the study of diffuse scattering from Ni/C multilayer mirrors at annealing [16] we also have observed this effect. The last study can be a conclusive proof that the discussed phenomenon is not a sequence of the experimental setup. During the annealing of a mirror in this experiment, the incoming Bragg-enhanced diffuse scattering line disappeared though the peak reflectivity of the mirror stayed quite high (10–30%). It is interesting that the degradation of incoming Bragg-enhanced diffuse scattering was accompanied by the mosaic-like spread of specular reflection. Also we have studied the effect asymmetry of incoming and outgoing Bragg-enhanced diffuse scattering from various multilayers and superlattices. As a result the following rules were revealed: 1. This effect is very important if the float glass or silica wafers are used, whereas in cases when single crystals were used as substrates this effect is

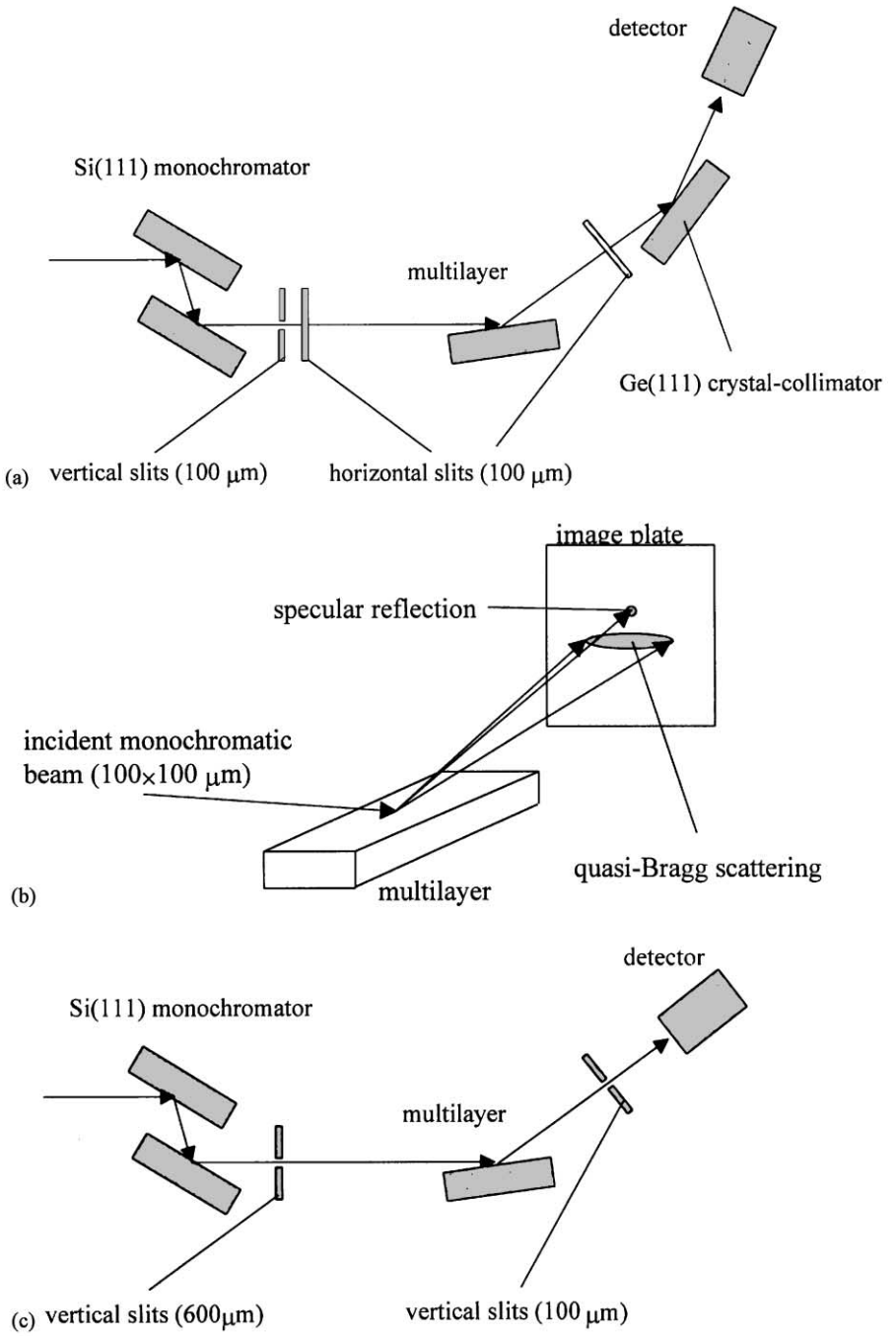

Fig. 4. The experimental setup: (a) the conventional triple-axis geometry with additional horizontal slits; (b) the experimental scheme with an image plate; (c) the slit geometry.

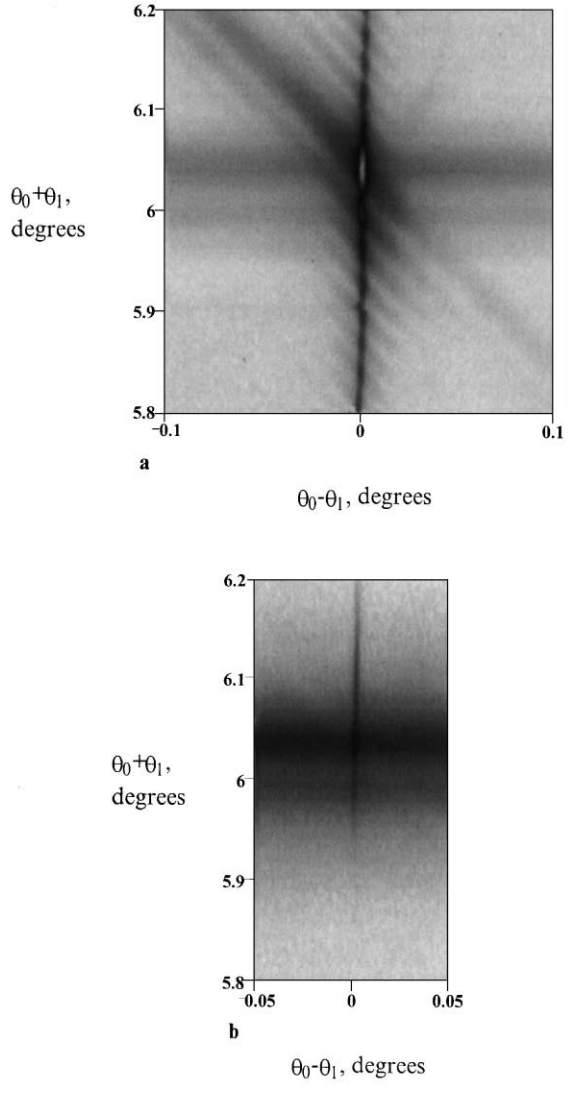

Fig. 5. The diffraction space maps of the first order Bragg reflection: (a) the conventional geometry; (b) the diffuse scattering in the specular diffraction plane was cut off by the slits.

remarkably smaller. 2. The asymmetry degree is more clear if the incident angle is smaller, for example, this asymmetry is very fine near the Bragg reflection satellites from a superlattice in the high-angle range. 3. The typical intensity dependence of incoming Bragg-enhanced diffuse scattering on standing wave localization is invisible.''

Another diffraction space map of the same Bragg reflection is shown in Fig. 5b. The main experimental condition difference between the data in Figs. 5a and b is that the specular diffraction plane was cut off by the horizontal slits in the latter case. As it is well seen from Fig. 5, the incoming Bragg-enhanced strip disappears, which means that the major part of this scattering occurs in the specular diffraction plane. The total disappearance of the incoming and outgoing Bragg-enhanced diffuse scattering strips can be explained by the limited dynamic range.

Our possible explanation of this phenomenon is the distortions of the coherent wave front caused by the macroscopic roughness imperfections with large length (flatness). Indeed, the diffracted X-rays do not ''sense'' these imperfections if their lengths are more greater than the Bragg extinction length (a few μm). From this point of view, the multilayer structure is ideal. Nevertheless, the distortions of the coherent wave front cause the off-specular scattering. In this case, the role of the Bragg diffraction is very simple: there is a reflection if the incident angle is equal to the Bragg one, otherwise, there is no reflection.

Such diffuse scattering mechanism makes the directions in and normal to the specular diffraction plane non-equivalent. A small incident angle results in different sizes of the irradiated sample square in these directions. If the size of coherent beam was about 2 μm in the direction normal to the specular diffraction plane, then in the specular diffraction plane the size of the coherently-irradiated sample square increased up to the value about a few mm. The result is that the diffuse scattering is located in the specular diffraction plane. The suggested interpretation explains well the dependence of the asymmetry degree of the incoming and outgoing Bragg-enhanced diffuse scattering on the incident angle. Indeed, the greater the incident angle, the finer is the effect discussed.

A situation paradox must be noted. If the incident wave would be completely plane and coherent, then the incoming Bragg-enhanced diffuse scattering would not be concentrated in the specular diffraction plane. Nevertheless, under real conditions, if the transverse coherent length is greater, then this effect can be observed clearly.

It is interesting to mark that the incoming and outgoing Bragg-enhanced strips disappear

completely due to the insufficient dynamic range of the detector system, whereas the quasi-specular scattering remains to be visible.

As an example of the importance of the transverse coherent length, a diffraction space map of the same sample and Bragg reflection obtained at another experimental setup is shown in Fig. 6. In this case the additional horizontal slits were removed, and the secondary crystal-collimator was replaced by secondary vertical slits; in so doing its thickness (100 μm) was six times smaller than the thickness of the primary vertical slits (600 μm). It should be noted that this "square grid" view can be observed near the Bragg reflection only. Away from the Bragg reflections, the scattering profiles become usual.

As for the $q_\perp$-dependence of the outgoing Bragg-enhanced diffuse scattering, which is very slightly visible in Fig. 5a, it was verified to have the same behavior as in the case of quasi-Bragg scattering.

4. Quasi-Bragg scattering

The diffraction space map from the W/Si multilayer mirror obtained by the use of an image plate is presented in Fig. 7. The upper spot in the figure is the specular reflection, and the central halo is the quasi-Bragg scattering sheet.

In Fig. 8 the quasi-Bragg scattering intensity versus the $q_\perp$-momentum transfer obtained from this experiment is compared to the quasi-Bragg intensity versus the momentum transfer in the specular diffraction plane, $q_\parallel$. The latter data were obtained using usual scans in the specular diffraction plane. As in Ref. [9], at high azimuthal angles, the quasi-Bragg scattering intensity is in good

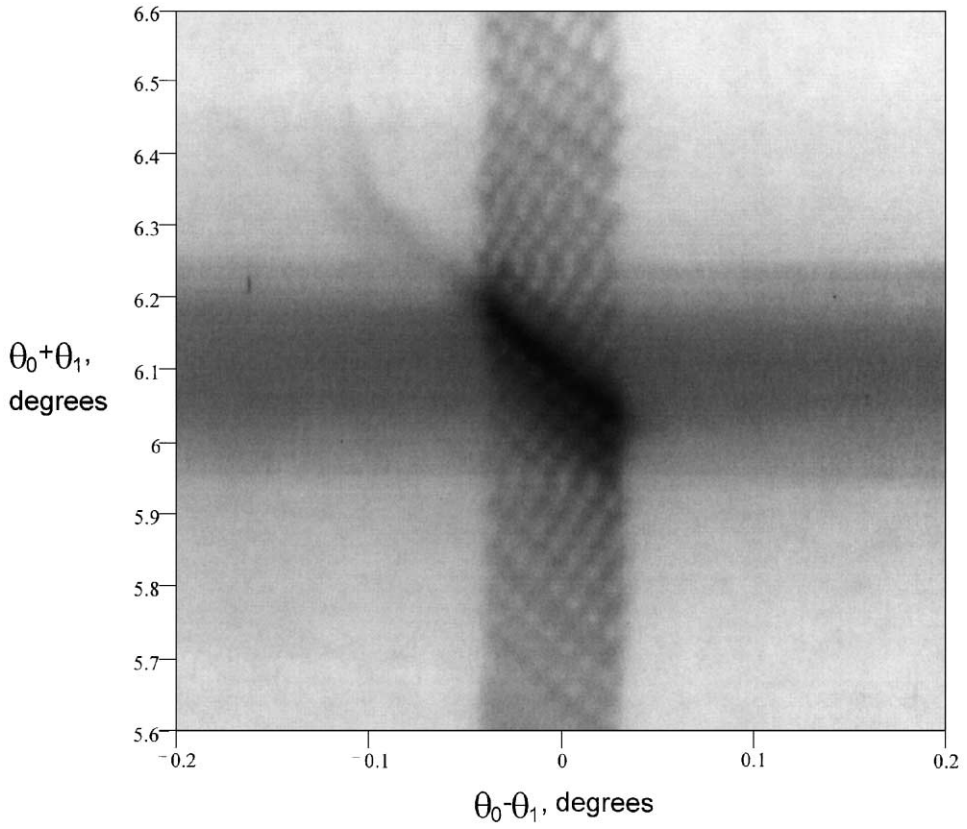

Fig. 6. The diffraction space map obtained by the use of the slit experimental setup (Fig. 4c).

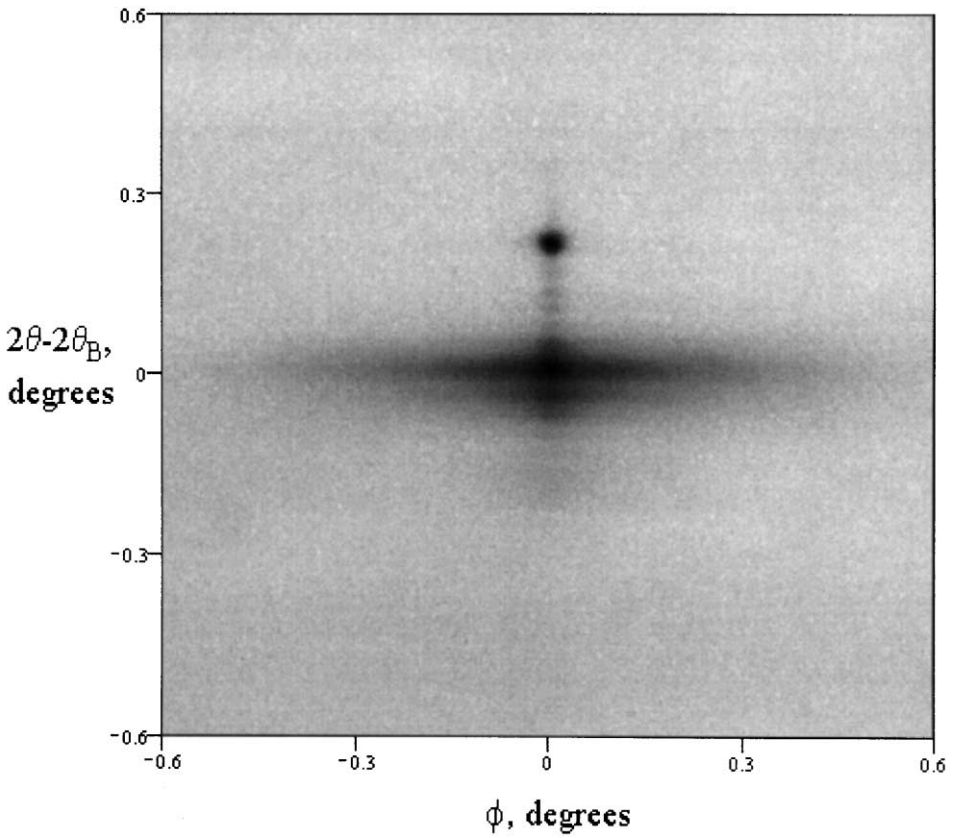

Fig. 7. The diffraction space map of diffuse scattering from the W/Si multilayer obtained with the use of an image plate: the incident beam sizes are $100 \times 100\,\mu m$, the distance from the scattering point to the image plate is 520 mm, ϕ is the azimuthal angle, 2θ and $2\theta_B$ are the total and double Bragg angles, respectively.

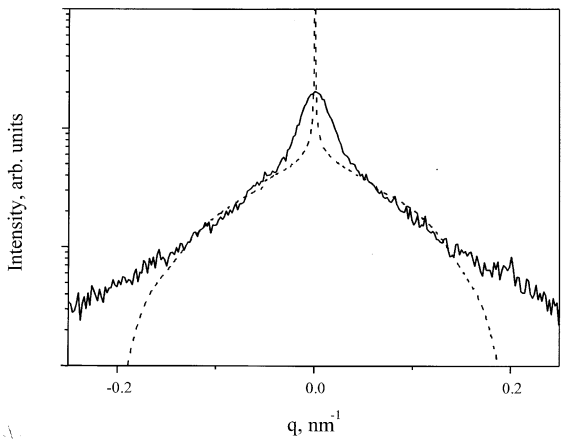

Fig. 8. The diffuse scattering intensities versus the momentum transfer: the solid curve is normal to the specular diffraction plane, $q_\perp$; the dashed curve is in the specular diffraction plane, with integration over ϕ, $q_\parallel$. The logarithmic intensity scale was used.

agreement with the theory with height–height self-correlation function (6). Nevertheless, additional diffuse scattering near the specular diffraction plane is well observed. A similar effect was observed in Ref. [9]. This feature was called "resolution dominated region" in this work. In order to remove any doubts, the scattering profiles of the quasi-Bragg scattering and specular reflection, whose width is determined by the angle resolution, are shown in Fig. 9. This Figure demonstrates well that the angle resolution is sufficiently better than the width of the quasi-Bragg scattering profile.

Thus, the data obtained support the existence of the roughness imperfections that are unlimited in some lateral directions. Moreover, the scattering from these imperfections can dominate as well observed from Fig. 9.

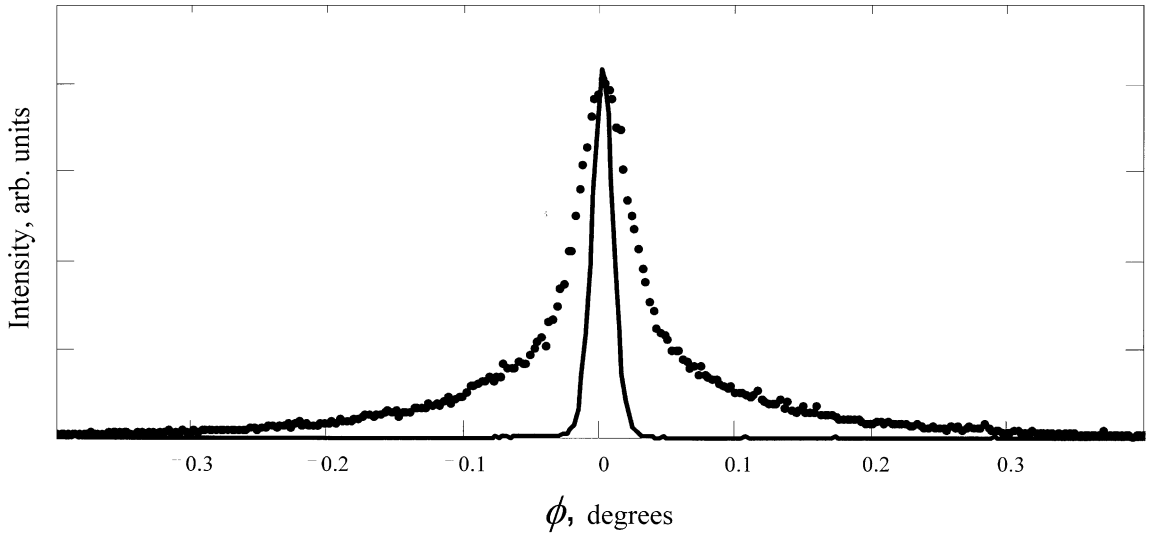

Fig. 9. The ϕ-profiles of the quasi-Bragg scattering (points) and specular reflection (solid curve) were shown using a linear scale. The width of specular reflection demonstrates the experimental angle resolution.

5. Conclusion

As a result of this study, two facts were revealed:

1. Additional diffuse scattering from the multilayer, concentrated in the specular diffraction plane, was observed when the incident angle was approximately equal to the Bragg angle.
2. The existence of the interfacial roughness imperfections, which are unlimited in some lateral directions, was shown. Moreover, the scattering from these roughness imperfections can dominate over the scattering from the conventional roughness described by correlation function (6). As a result, quasi-Bragg as well as other types of diffuse scattering were observed to have tendency to concentrate near the specular diffraction plane.

Acknowledgements

We would like to thank the staffs of VEPP-3, optical workshops, and SSRC at BINP for their assistance. We are grateful to A.Artushin for the useful discussions. This study was supported by the Russian Foundation for Basic Research, Grants Nos. 99-02-16671 and 00-02-17624.

References

[1] J.B. Kortright, J. Appl. Phys. 70 (1991) 3620.
[2] D.E. Savage, J. Kleiner, N. Schimke, Y.-H. Phang, T. Jankowski, J. Jacobs, R. Kariotis, M.G. Lagally, J. Appl. Phys. 69 (1991) 1411.
[3] V. Holy, J. Kubena, I. Ohlidal, K. Lischka, W. Plotz, Phys. Rev. B 47 (1993) 15896.
[4] V. Holy, T. Baumbach, Phys. Rev. B 49 (1994) 10668.
[5] M. Kopecky, J. Appl. Phys. 77 (1995) 2380.
[6] D.G. Stearns, J. Appl. Phys. 71 (1992) 4286.
[7] A.V. Andreev, A.G. Michette, A. Renwick, J. Modern Opt. 35 (1988) 1667.
[8] A.V. Vinogradov, private communication.
[9] T. Salditt, T.H. Metzger, J. Peisl, Phys. Rev. Lett. 73 (1994) 2228.
[10] S.K. Sinha, E.B. Sirota, S. Garoff, H.B. Stanley, Phys. Rev. B 38 (1988) 2297.
[11] N.V. Vostokov, S.V. Gaponov, V.L. Mironov, A.I. Panphilov, N.I. Polushkin, N.N. Salashenko, A.A. Fraerman, M.N. Haidl, Proceedings of the X-ray Optics 2000 Conference, Nijnii Novgorod, Russia, 2000 (in Russian).
[12] L.G. Parrat, Phys. Rev. 95 (1954) 359.
[13] Brief Description of the SR Experimental Station, Preprint, INP, 90–92, Novosibirsk, 1990.
[14] A.V. Andreev, JETP 83 (1996) 1162.
[15] E.A. Kondrashkina, S.A. Stepanov, R. Opitz, M. Schmidbauer, R. Kohler, R. Hey, M. Wassermeier, D.V. Novikov, Phys. Rev. B 56 (1997) 10469.
[16] V.A. Chernov, E.D. Chkhalo, N.V. Kovalenko, S.V. Mytnichenko, Nucl. Instrum. and Meth. A 448 (2000) 276.